38

ELECTRONIC STRUCTURE OF CONDUCTING π-ELECTRON SYSTEMS*

P. M. GRANT and INDER P. BATRA

IBM Research Laboratory, San Jose, California 95193 (U.S.A.)

Summary

We will discuss the application of one-electron band theory to several systems where π-electron delocalization has been experimentally established. We will use polyacetylene as our prototype and extend results on it to related polymers such as $(SN)_x$, polypyrrole and poly(p-phenylene). We will particularly concentrate on those aspects of chemical bonding and symmetry which govern whether a given system will be semiconducting or metallic, and which scale its transport properties.

Interest in the fundamental electronic properties of linear π-electron systems with extended conjugation is historically grounded in two related areas of physical chemistry, one experimental and the other theoretical. The first of these encompasses the spectroscopy of dyes and polyenes, as initially characterized by Brooker [1], and the second arises from quantum chemical investigations of extended hydrocarbon chains originally begun by Longuet-Higgins and Salem[2] and since continued by many other workers [3 - 7]. The accounting for properties discovered optically in these systems by models proposed theoretically is still an ongoing process.

From the viewpoint of solid state physics, it has long been recognized that the wavefunctions of extended π-electron systems are likely to be quite delocalized, thus holding out the promise of high carrier mobility under conditions of partial occupancy of these eigenstates. Graphite, of course, is the quintessential example of such a system. One of the most fascinating aspects of this delocalization in polymers is that it would be confined primarily to one dimension, as opposed to the conventional three-dimensional itinerant electron systems found in the usual metals and semiconductors. In recent years, non-polymer, one-dimensional systems (more correctly termed quasi-one-dimensional), as epitomized by the charge transfer salts of TCNQ, have been extensively studied and a great richness of phenomena uncovered. The

---

latest in the family of highly anisotropic materials are the conducting and semiconducting organic polymers. These materials, in their intrinsic state, are medium band gap ($E_G \sim 1$ - 3 eV) semiconductors, which, when partially oxidized or reduced by external reagents, become quite highly conducting ($\sigma \sim 1$ - $1\,000\ \Omega^{-1} \cdot cm^{-1}$) [8 - 13]. Some of their more interesting attributes include the possibility of a metal–insulator transition at critical dopant levels [14] and the question of current conduction by the propagation of bond defects [15 - 17].

In this paper, we will dwell on the applicability of conventional one-electron concepts to questions of the transport and optical properties of such extended π-systems, and how these concepts relate to chemical interactions between constituent atoms and molecules. Figure 1 depicts the polyacetylene polymer structures we will implicitly have in mind as our prototypes throughout the following discussion. These two configurations of polyacetylene, especially the *trans*-form, provide the basic conceptual foundation for the physics of all π-bonded polymers in general. Now, the one electron approach is in contrast to the quantum mechanical treatment of chemical species using Complete Neglect of Differential Overlap (CNDO) with Configuration Interaction (CI), Pariser–Parr–Pople (PPP), or Hubbard techniques in which the interaction between constituent molecular electrons, that is, correlation or Coulomb repulsion/attraction in both the ground and excited states, is explicitly considered [18 - 20]. Our belief that these interactions may be small with respect to electronic kinetic energy in conjugated polymers is motivated by experience with π-bonded inorganic systems such as graphite and $(SN)_x$ where it has been found, both theoretically and experimentally, that Coulomb interactions play a secondary role. Reinforcing these expectations is the very high conductivity, with implications of high microscopic mobility, found in oxidized or reduced polyacetylene. On the other hand, we do not mean to imply that Coulomb effects can be completely ignored, especially in the area of optical phenomena.
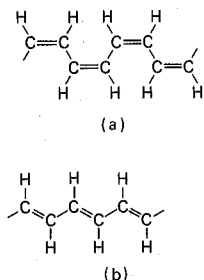

(a)

(b)

Fig. 1. Schematic of the chain structure of (*a*) cis-polyacetylene; (b) *trans*-polyacetylene.

We begin by considering the complete electronic Hamiltonian for a system of atomic or molecular sites in the Born–Oppenheimer approximation, each contributing a single π-electron:

$$H = \sum_{i=1}^{N} \left\{ \frac{p_i^2}{2m} + V(\vec{r}_i) + \sum_{j>i}^{N} \frac{e^2}{|\vec{r}_i - \vec{r}_j|} \right\}, \tag{1}$$

where the first term is the usual kinetic energy (delocalization) part, the second term the potential energy of the i-th π-electron arising from the electrostatic field of all sites combined, and the third the electrostatic interaction of all π-electrons amongst themselves. The sum on i, j ranges over all N sites, in principle infinite for an infinite polymer chain. Even given the power of modern digital computers, the direct numerical solution of the eigenproblem associated with eqn. (1) is still beyond reach. It is doubtful that such a solution would provide great physical insight even if it were possible. By treating eqn. (1) in various approximations, one can recover most of the essential physical and chemical interactions that are subject to measurement. The approximation we will employ, the one-electron approximation, consists in replacing the third term in eqn. (1) by the potential energy the i-th π-electron possesses in the average electrostatic field of all the others computed under restrictions imposed by the Pauli principle. This simplification reduces eqn. (1) to a single electron Hamiltonian and of course forms the physical basis for the well-known Hartree–Fock self-consistent field method. The sum total of all differences between Hartree–Fock and experimental energies defines the correlation energy. The third term of eqn. (1) then becomes the sum of an average Coulomb potential plus an "exchange" term arising from the eigenstate occupancy constraints imposed by the Pauli principle. The former interaction augments the Coulomb field arising from nuclear charges while the latter introduces a non-classical potential, whose ramifications we will discuss shortly. It is important to point out that all simpler one-electron techniques on down to the Hückel empirical molecular orbital approach are motivated philisophically by the Hartree–Fock approximation. The usefulness of the one-electron approximation in discussing π-conjugated polymer systems (and any other extended electronic system for that matter) lies in giving a positive answer to the following two questions:

(1) Does the addition or subtraction of an electron from the polymer π-system leave its one-electron eigenstates essentially unchanged?

(2) Do optical excitations between filled and empty one-electron states result in free, or at least weakly bound, electron–hole pairs?

The first question deals with the change in the electron count brought about by oxidation or reduction of the polymer chain or by photoemission processes, while the second addresses whether stable excitons can be created by optical excitation. If it turns out that the one-electron eigenstates of a given polymer structure are very delocalized, then it is easy to see that the answer to both questions should be affirmative. In the language of either solid state or molecular quantum theory, one says that Koopman's Theorem is obeyed. Given that the electronic wavefunctions are found to be extended over the polymer backbone, very minimal Coulomb interaction should be expected. In this situation, the single particle linear momentum is conserved and

appears as an important quantum number and we become encouraged to employ solid state band theory in the one-electron approximation as the appropriate theoretical framework.

However, having said all this, we must point out that the situation in practice is not so simple. Our two questions above are more profound than they may at first appear and constitute essential probes of a real understanding of the physics of extended systems. One might expect that an *ab initio* Hartree–Fock calculation would provide the best possible one-electron estimate of the polymer eigenstates. In fact, when such calculations are performed, the results are in very poor agreement with experimental bandwidths and band gaps. For example, the Hartree–Fock band gap for *trans*-$(CH)_x$ is found to be around 7 eV [5], whereas the experimental number is nearer 1.5 eV. On the other hand, if one uses the so-called local exchange approximation [21], in which the Hartree–Fock exchange potential is replaced by a cube-root dependence on the local charge density, one finds unexpectedly good agreement with experiment. The problem lies in the fact that the Hartree–Fock approximation, by virtue of its neglect of correlation amongst electrons *in the filled valence levels* (as opposed to correlation arising from excitations to virtual states, which is also neglected), overestimates the long-range effects of exchange. This is a well-known paradox every student of solid state physics encounters when attempting to apply the Hartree–Fock approximation to the free electron gas. The addition of correlation to the ground state tends to screen the long-range part of the Hartree–Fock exchange potential. It turns out that the local exchange approximation fortuitously contains the physics of this screening and forms a much better model interaction than the seemingly more rigorous Hartree–Fock approach. This screening acts to reduce both the bandwidth and band gap from their Hartree–Fock values to magnitudes usually slightly below experimental results. To carry our discussion of these points further would take us beyond the scope of this paper. The interested reader is referred to papers by Overhauser [22] and Kunz and Collins [23] for a more complete examination of correlation in the one-electron model. We close our remarks here by reiterating that ground state correlation effects are sufficiently well incorporated into the one-electron approximation by the local exchange potential used in the calculations to be discussed hereafter.

The relationship between fundamental chemical and band theoretic concepts are illustrated in Figs. 2 and 3. The equations in the left-hand column of Fig. 2 are familiar from the Hückel MO model for cyclic molecules of $2N$ atoms. This model is isomorphic to a finite length linear polymer with cyclic boundary conditions. As the chain length or number of constituent atoms, $2N$, increases, the density of eigenstates becomes, for all practical purposes, continuous and we pass over to counting states in momentum space as shown in Fig. 2. The one-electron parameters, α, the "Coulomb integral", and β, the "resonance integral" (termed in solid state physics the "transfer integral"), separable from eqn. (1) in the Hartree–Fock approximation, thus provide the link between the chemistry and solid state physics
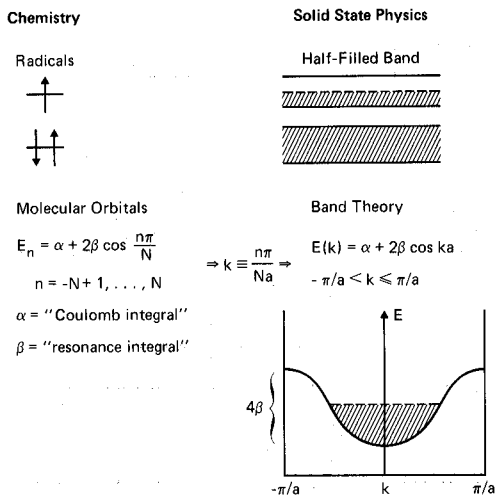
Chemistry   **Solid State Physics**

Radicals   Half-Filled Band

Molecular Orbitals   Band Theory

$E_n = \alpha + 2\beta \cos \dfrac{n\pi}{N}$ $E(k) = \alpha + 2\beta \cos ka$

$\quad n = -N+1, \dots, N$ $\quad -\pi/a < k \leqslant \pi/a$

$\Rightarrow k \equiv \dfrac{n\pi}{Na} \Rightarrow$

α = "Coulomb integral"

β = "resonance integral"

4β

$-\pi/a \qquad k \qquad \pi/a$

Fig. 2. Comparison of chemical and solid state physics concepts on the origin of metallic behavior.

Chemistry   **Solid State Physics**

Closed Shells   Filled Bands

E_G

$-\pi/a \qquad k \qquad \pi/a$

Radical Chain   Wigner Lattice
(Weak Overlap)
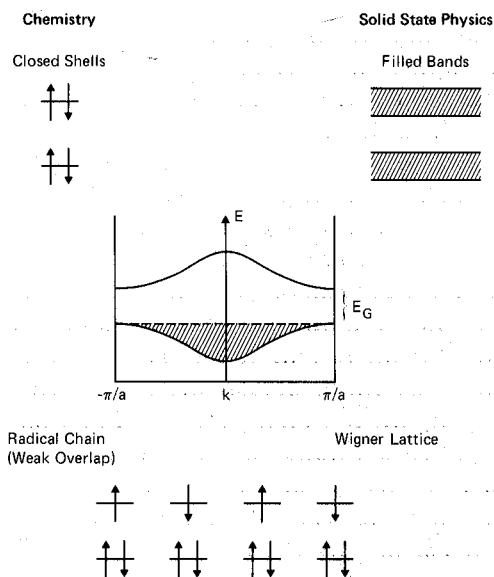
Fig. 3. Origin of the insulating state from chemical and solid state viewpoints.

of polymers. We will see shortly that β contains all the dynamical properties of the mobile electrons and holes in polymers.

Whereas Fig. 2 demonstrates the emergence of metallic behavior in an infinite polymer whose basic units are radicals, Fig. 3, on the other hand, depicts the origin of the insulating state for a system where the repeat unit contains an even number of electrons (closed shell). Thus, the number of electrons in the constituent molecules, and their internal symmetry arrange-

ment in the polymer unit cell, give an important prediction of the solid state properties of the infinite chain in the one-electron model. On the other hand, if the overlap of the π-orbitals is small (small β), then nearest neighbor Coulomb repulsion forces will tend to localize the electrons on molecular sites forming an insulating "Wigner lattice" of spins. The one-electron theory now no longer applies, and a spectral gap appears which represents the energy necessary to promote an electron from one molecular unit to its neighbor. This picture is very analogous to the singlet transitions so well known in organic molecules, except that now the charge-transfer process takes place between two molecules rather than within an individual species. If we can think of gradually increasing the π-overlap, say by continuously decreasing the chain repeat length, there arises a distance where the electrons can screen their mutual Coulomb repulsion forces and delocalization will spontaneously occur. This discontinuous change from the insulating to the metallic state in an odd-electron system has come to be known as the Mott–Hubbard transition. The ensuing screening effect is the prime physical reason why one-electron models work so well, as argued earlier, even when the density of electrons approaches 10^{23} per mole, a typical value for a conventional metal.

The dynamical properties of an electron moving along a polymer chain are described in band theory by the effective mass concept. This concept prescribes that electrons and holes *localized in momentum space* near band extrema can be treated as classical particles whose kinetic energy quadratically depends on their quasi-momentum, $\hbar k$. Simply expanding the dispersion equation in Fig. 2 to first order at $k = 0$ or $k = \pi/a$ verifies this assumption. Applying elementary Newtonian mechanics to such particles leads to the following expression for the effective mass:

$$m^* = \hbar^2 (d^2 E/dk^2)^{-1}. \tag{2}$$

Classical particles with this mass moving in an electric field and subject to damping by scattering processes will have their conductivity given by

$$\sigma = Ne^2 \tau/m^*, \tag{3}$$

where N is the total number of free carriers and τ is the scattering rate from, for example, chain vibrations and/or defects. Using the relation $E(k) = \alpha + 2\beta \cos ka$ from Fig. 2, eqn. (2) gives

$$|m^*|_{min} = \hbar^2/2\beta a^2 \tag{4}$$

for the minimum magnitude of the effective mass. We see that the larger is β, the smaller is $|m^*|$ and thus the more mobile are the carriers. In Fig. 4, we have plotted the value of β for the overlap of $C(2p)$ π-orbitals calculated in the Mulliken–Wolfsberg–Helmholtz (MWH) [24] approximation as a function of interatomic distance. The figure shows the bounds imposed by the extremes of single and double bond order. We note that β ranges from 2.4 to 3.2 eV. These values are very large when compared with other organic compounds commonly considered to be conductors or semiconductors. For example, in molecular crystals like anthracene or polyvinylcarbazole, the
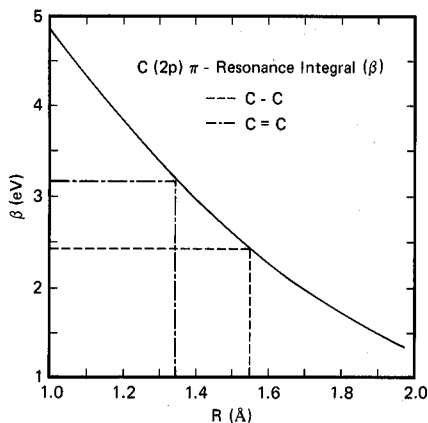
Fig. 4. Values of the resonance integral computed in the MWH approximation between C(2p) π-orbitals as a function of bond length. The distances corresponding to single and double bond distances are indicated. In the MWH approximation, the resonance integral, β, is given by $\beta = 0.75 \, I_\pi S_{\pi\pi}$, where I_π and $S_{\pi\pi}$ are the ionization potentials and $\pi-\pi$ overlap for C(2p) levels, respectively.

intermolecular resonance integrals are at best a few thousandths of an eV, [25], and even in the (TTF)(TCNQ) family of conducting charge-transfer salts they reach only 0.4 - 0.8 eV [26, 27]. On the other hand, in the inorganic superconducting polymer $(SN)_x$, the resonance integral between S(3p) and N(2p) on neighboring atoms is around 2.5 eV [28]. Table 1 summarizes these data. The similarity between π-electron overlaps within $(SN)_x$ and those within $(CH)_x$ is a strong motivating factor for applying one-electron theory to the latter family of compounds.

In Fig. 5, we show the dependence of $m*$ on bond length, as found from eqn. (4) and Fig. 4. In accord with the relatively large β, the effective mass magnitude is far less than that usually encountered in most organic compounds, and approaches values associated with inorganic covalent semiconductors such as II - IV compounds where $|m*/m| \sim 0.3$. It is interesting to see that the variation in $m*$ with bond length is quite small. This is due to the fact that any increase in β is necessarily accomplished by a decrease in a^2 and results in a partial cancellation of the changes in β within eqn. (4).

In the solid state, factors other than nearest neighbor chemical bonding interaction must also be considered. We have already pointed out the importance of electron count in determining whether a given chain system will have ground state conducting or insulating properties. Equally important is the internal symmetry arrangement of the constituent atoms and molecules in the polymer unit cell and this symmetry must be allowed for in performing the electron count. Figure 6 illustrates the situation for hypothetical uniform bond length $trans$-polyacetylene. Consider each dot to represent the π-electron associated with each CH molecule. A simple electron count gives two π-electrons per unit cell, thus, by our previous arguments centered on Figs. 2 and 3, uniform bond $trans$-$(CH)_x$ should be an insulator. However, it

TABLE 1

Values of the resonance integral (β), effective mass ($m*$), and
band gap (E_G) for various organic crystals and polymers
($\parallel$, $\perp$ refer to the chain axis or direction of high conductivity.)

Compound	β (eV)	$\|m*/m\|$	E_G (eV)
Anthracene	2.5×10^{-3} [a]	11 [b]	3.9 [c]
(TTF)(TCNQ)	0.15 ($\parallel$) [d] 1.7×10^{-3} ($\perp$) [d]	2.5 [e]	0 - 0.1 [f]
(SN)$_x$	2.50 ($\parallel$) [g] 0.25 ($\perp$) [g]	1.0 [g] 2.0 [g]	0 [h]
trans-(CH)$_x^i$	3.00 ($\parallel$)	0.5	1.4 [j]
cis-(CH)$_x^i$	2.60 ($\parallel$) 0.10 ($\perp$)	0.5	1.1
Polypyrrole[i]	3.00 ($\parallel$)	0.5	2.5
Poly(p-phenylene)[i]	2.00 ($\parallel$)	0.5	2.0

[a] Ref. 25 (computed).
[b] D. M. Burland and V. Konzelmann, *J. Chem. Phys.*, 67 (1977) 319.
[c] D. M. Hanson, *CRC Critical Reviews in Solid State Sciences*, April, 1973, p. 243.
[d] Ref. 26 (computed).
[e] A. J. Berlinsky, J. F. Carolan and L. Weiler, *Can. J. Chem.*, 52 (1974) 3373 (computed).
[f] D. B. Tanner, C. S. Jacobsen, A. F. Garito and A. J. Heeger, *Phys. Rev. Lett.*, 32 (1974) 1301.
[g] Ref. 28 (computed).
[h] Ref. 38 (computed).
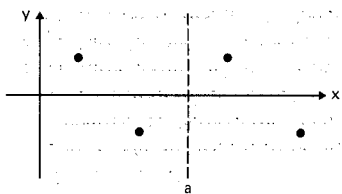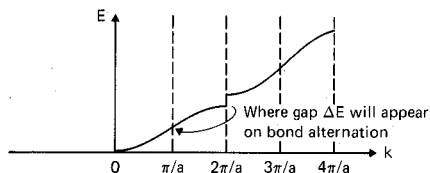[i] Present work (computed).
[j] Ref. 29.
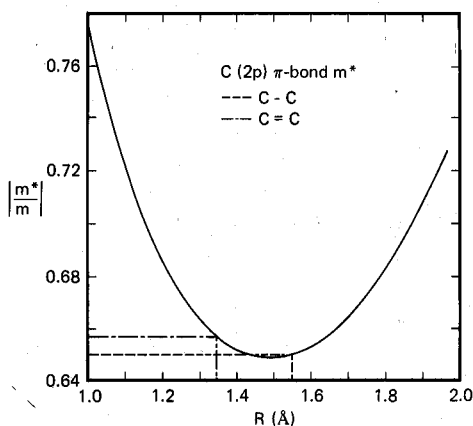
Fig. 5. Effective mass ratio with respect to free electrons calculated from the π-resonance integrals of Fig. 3.

Screw Symmetries & Band Structure

Translation: $V(x, y) = V(x - a, y)$
Screw: $V(x, y) = V(x - a/2, -y)$

Plane Wave Representation in Second Order
Degenerate Perturbation Theory

$\Delta E \cong 2 \, |V \, (K)| = 2 \, |\Delta\beta|,$

$K = \dfrac{2\pi}{a} n; \, n = 0, \pm1, \pm2, \ldots$

For screw axis symmetry, $V(odd) \equiv 0$

Fig. 6. Effect of polymer unit internal symmetries on its band structure. This Figure indicates how band gaps are produced on moving from uniform bond to alternating bond structures ($\Delta\beta = \beta_1 - \beta_2$).

can be seen that a half-cell translation followed by an inversion through the y–z-plane is a symmetry operation for this particular chain. The implications of the presence of this "screw axis" symmetry will now be addressed.

In the lower half of Fig. 6, we show another way of looking at band theory. Our previous discussion revolved around using linear combinations of atomic orbitals as the basic function framework and considering the effect of nearest neighbor overlap in producing delocalized bands. It is perfectly plausible to approach band theory from a diametrically opposite point of view; that is, to assume complete delocalization as a starting point with plane waves as the unperturbed representation and to consider the effect of "turning on" the atomic or molecular potential as a small perturbation. The physical picture is then one of particle waves scattering inelastically from a periodic array of rigid centers, much in the manner of inelastic X-ray scattering. As with X-rays, we can define a reciprocal lattice upon which the electronic quasi-momentum is quantized. The lattice points corresponding to momenta at which the electrons will undergo inelastic scattering are given by the coefficients of the chain periodic potential when expanded as a Fourier series on the reciprocal lattice. The physical origin of the energy loss on scattering can be conceived as arising from bonding–antibonding transitions associated with the constituent molecules. Generally there will be a finite

potential coefficient at each reciprocal lattice point giving rise to an energy gap in the energy–momentum dispersion. Often, however, as a result of high symmetry within the unit cell, certain of the potential coefficients (structure factors) will remain zero and no gap will emerge where one might have been expected on the basis of translational symmetry alone. Such is the case for uniform bond $trans$-$(CH)_x$ as shown in Fig. 6. There is no gap at $k = \pi/a$ where the Fermi level crosses the lower band. Thus, in the one-electron picture, uniform bond $trans$-$(CH)_x$ would be a metal.

On the other hand, there are a number of experimental indications that $trans$-$(CH)_x$ is a semiconductor with a band gap of roughly 1.5 eV [29, 30]. In the one-electron model, the presence of bond alternation removes the screw symmetry operation of Fig. 6 and results in the production of a Fourier potential coefficient, and, hence, the creation of a gap, at $k = n\pi/a$ where n is an odd integer. This result is simply the solid state physics confirmation of the free electron molecular orbital picture introduced long ago by Kuhn [31]. After the introduction of Kuhn's model, confusion apparently existed for a while over the physical necessity for bond alternation in closed shell polyenes. There seemed to be no obvious driving force to produce such a "pseudo-Jahn–Teller effect". After all, if a cyclic system, such as benzene, possesses two resonant structures with the same energy, the equilibrium configuration should be their average, that is, one with equal bond lengths. It is here that band theory provides very useful insight. We have seen that uniform bond $trans$-$(CH)_x$ should be a metal. Peierls and others [32] have shown that the metallic state in one-dimension is inherently unstable and that the slightest degree of bond alternation will mix states just above and below the Fermi level crossing at $k = \pi/a$ producing a gap thus lowering the ground state energy of the π-system at the expense of a smaller increase in energy due to σ-compression. This state mixing gives rise to the required Fourier potential components discussed above. The whole process can be thought of as a solid state manifestation of the Jahn–Teller effect. The reason such distortions do not occur in low molecular weight ring compounds like benzene is that the excited state that carries the requisite symmetry lies 4 eV away from the ground state and so the coupling is very small. However, in the higher molecular weight annulenes, this excited state is much closer and a tendency toward distortion arises [35]. The details of the Peierls argument from a quantum chemical viewpoint are elegantly presented in the book by Salem [35].

The effect [6] of bond alternation on the energy bands of one-dimensional $trans$-$(CH)_x$ can be seen in Fig. 7. We will not here go into the calculational details since these are adequately covered in ref. 6. It is sufficient to say that the technique employed is frontier state-of-the-art Linear Combination of Atomic Orbitals (LCAO) Extended Tight Binding (ETB) [39]. No empirical parameters, other than the atomic coordinates and the Slater local exchange parameter, were used. As indicated in Fig. 7, atomic coordinates pertaining to three different bond lengths were employed. It should be stressed that the crystallinity of $trans$-$(CH)_x$ is currently not high enough to
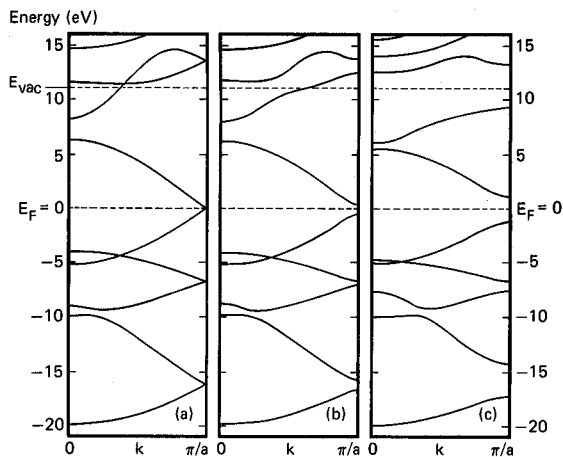
Fig. 7. Band structure of one-dimensional *trans*-(CH)$_x$ for three choices of bond length: (a) uniform (1.39 Å); (b) weakly alternating (C=C: 1.36 Å, C–C: 1.43 Å); and (c) strongly alternating (C=C: 1.34 Å, C–C: 1.54 Å). Note the lifting of the degeneracy at E_F, thus progressing from the metallic to the insulating state, with the onset of bond alternation (reproduced from ref. 6).

permit the experimental structural determination of actual bond lengths. The left-hand panel (a) shows the result for equal bond lengths, the center (b) for bond lengths equal to those used in the calculations of Andre and Leroy [4] and which are typical of values found in long polyene molecules, and finally the right-hand panel (c) was computed for single and double bond lengths taken from ethane and ethylene, respectively. We see that Fig. 7 verifies our qualitative picture outlined above. The most important feature to be noted is the strong dependency of the band gap on the amount of bond alternation, with a maximum value of 2.3 eV obtained for complete alternation.

If we generalize the simple model of Fig. 2 to a dimerized linear chain, as represented by alternate-bond *trans*-(CH)$_x$, we obtain for the band gap at the zone boundary $E_G = 2|\beta_1 - \beta_2|$ where β_1 and β_2 are the resonance integrals belonging to the two different bond lengths. We compute the respective resonance integrals using the MWH approximation, namely, $\beta = 0.75\,I_\pi S_{\pi\pi}$, where $S_{\pi\pi}$ is the π-overlap and I_π is the first ionization potential of C(2p) level. In Fig. 8 we plot the range of gaps obtained for bond length differences over the interval 1.34 - 1.54 Å, spanning single to double bond values. Because of the simplicity of the model, the gaps obtained are somewhat less than those from the LCAO–ETB calculation. In the absence of structural information, the choice of a "reasonable" bond alternation for *trans*-(CH)$_x$ is somewhat open. As mentioned above, the phototransport threshold would suggest a band gap of 1.5 eV. From our calculations, this would imply a bond alternation greater than the moderate value used to give the center panel (b) of Fig. 7. However, we believe this would be an overinterpretation
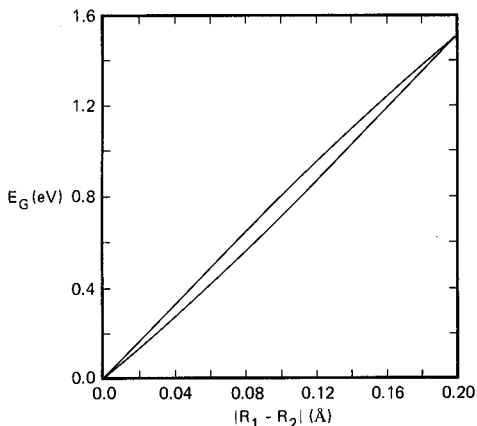
Fig. 8. Band gap for alternating *trans*-(CH)$_x$ as a function of absolute difference in bond lengths. The plot represents the contour enclosing all possible band gaps for the set of differences 1.34 Å $\leqslant \{|R_1 - R_2|\} \leqslant 1.54$ Å.

of our results. We only note that bond differences in extended polyenes such as the β-carotene family range from 0.05 - 0.15 Å at distances far from the chain ends and that our calculated gaps associated with these values bracket the experimental number for *trans*-(CH)$_x$.

Up to now we have considered a perfectly periodic alternating *trans*-(CH)$_x$ structure. Pople and Walmsley [15] have demonstrated that such a structure has a low threshold to the formation of defects, or interruptions, in bond alternation. That is, they find the energy required abruptly to produce two "single" bonds in a row to be several tenths of an eV. Su *et al.* [17] have reconsidered the ideas of Pople and Walmsley in a soliton formalism and estimate the neutral defect activation energy to be 0.4 eV for a band gap of 1.5 eV. As pointed out by Pople and Walmsley and Su *et al.*, such a defect should be electrically neutral with spin 1/2, and, upon ionization, become spinless and capable of carrying current. On the other hand, one should expect to find an activated magnetic susceptibility in undoped polyenes, and this behavior does not seem to be observed. Instead, a Curie law dependence is found [33, 34]. Perhaps a large number of Pople–Walmsley-like neutral defects are structurally frozen in during the polymerization process and these swamp out those that are activated [33]. All in all, the remark made by Salem [35] in 1965 that no satisfactory explanation for the e.s.r. in polyenes has been found, appears to remain valid.

For *cis*-(CH)$_x$, a reasonably good estimate of the probable crystal structure has been made by Baughman and coworkers [36] and is shown in Fig. 9. This estimate enables us to study in a general way the effects of interchain coupling on the transport properties of conducting polymers. The resulting band structure is shown in Fig. 10. The principal conclusions concerning the band structure of three-dimensional *cis*-(CH)$_x$ have been detailed previously [6]. We will only give here a summary.
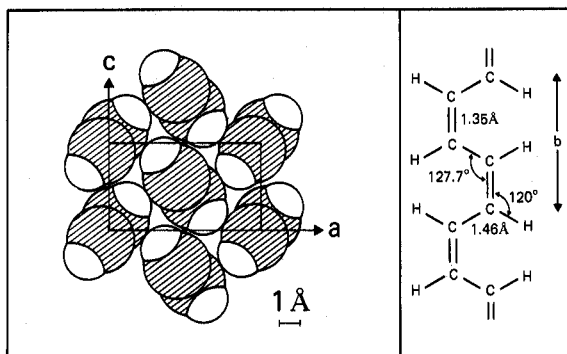
(CH)$_x$
Orthorhombic PRMA

a = 7.61Å
b = 4.47Å
c = 4.39Å

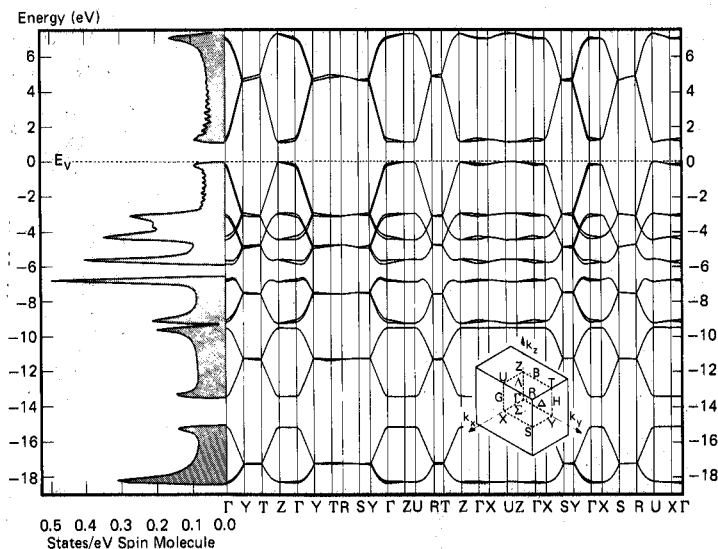Fig. 9. Probable crystal structure of *cis*-(CH)$_x$ deduced from the packing analysis of ref. 36.

Fig. 10. Band structure and density-of-states for three dimensional *cis*-transoid polyacetylene. The notation along the k-axis is the Bouckart–Smoluchouski–Wigner notation for the irreducible representations of the monoclinic space groups whose Brillouin zone is shown in the insert.

(1) The conduction and valence bandwidths are not materially different from *trans*-(CH)$_x$. Thus, the intrinsic transport properties of the two materials should be rather similar, as is indeed found experimentally.

(2) The maximum bandwidth in any given interchain direction is about 0.3 eV. On the scale of other quasi-one-dimensional materials, such as the charge transfer salts of TCNQ, this represents considerable interaction and

may act to suppress static charge density wave instabilities (*i.e.*, static Peierls distortions) which would otherwise have arisen on doping. That is, the tendency to form a superlattice governed by the position of the Fermi vector in the doped material would be offset by the large interchain interaction, as is the case in $(SN)_x$.

(3) Unlike *trans*-$(CH)_x$, the unit cell of *cis*-$(CH)_x$ always contains an internal screw axis symmetry operation regardless of whether bond alternations exists. As in uniform bond *trans*-$(CH)_x$, this symmetry operation results in the absence of gaps at several zone boundaries of *cis*-$(CH)_x$. However, in *cis*-$(CH)_x$ the bonding valence band is completely full due to the even number of electrons in the unit cell element undergoing the screw axis operation. Thus the calculated 1.2 eV band gap more or less arises from the difference in bonding–antibonding π-state energies in the (C_2H_2) molecule. There is thus no Peierls-like driving force to produce bond alternation in undoped *cis*-$(CH)_x$. Any bond length difference must be attributed to other sources.

It has been recognized for some time that $(CH)_x$ and $(SN)_x$ have strong structural and electronic similarities. Topologically, $(SN)_x$ rather resembles *cis*-$(CH)_x$, but electronically, because the SN unit is a radical and C_2H_2 is not, it is more analogous to uniform bond *trans*-$(CH)_x$. The proper complete analogy to $(SN)_x$, both structurally and electronically, would be the hypothetical compound *cis*-$([C_2H_2]^-)_x$. The crystal structure of $(SN)_x$ [37] is shown in Fig. 11 and its three-dimensional band structure [38] in Fig. 12. The practiced eye will recognize many similarities to Fig. 10, *cis*-$(CH)_x$, except that now the Fermi level passes near a zone boundary degeneracy for the very reasons discussed earlier in the case of uniform bond *trans*-$(CH)_x$. The states
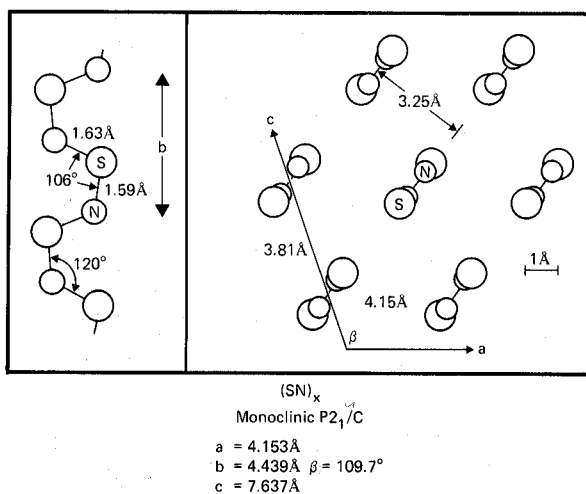

(SN)$_x$
Monoclinic P2$_1$/C

a = 4.153Å
b = 4.439Å β = 109.7°
c = 7.637Å

Fig. 11. Crystal structure of $(SN)_x$: (a) chain configuration along the monoclinic unit cell *b*-direction. Two unit cells are shown. (b) arrangement of chains shown stereographically projected on the *a–c* plane.
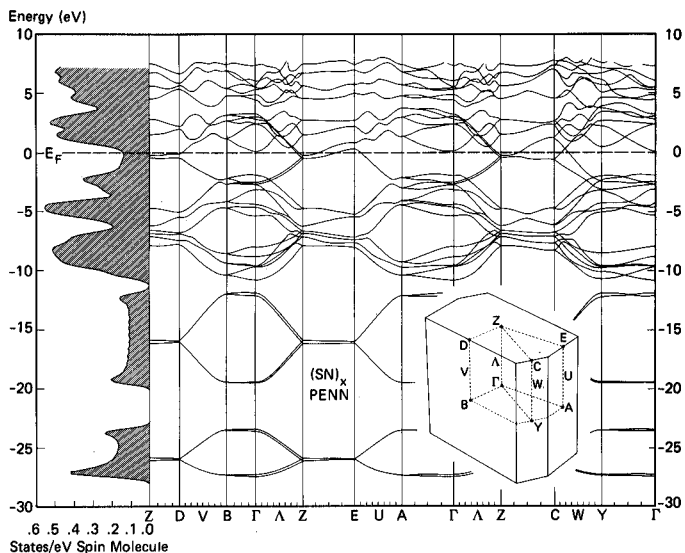
Fig. 12. Band structure and density-of-states for $(SN)_x$ (reproduced from ref. 38).

near this crossing are composed primarily of a π-mixture between S(3p) and N(2p) orbitals [39] in close analogy to the overlap of adjacent C(2p) states in $(CH)_x$. The most significant difference is that the degree of interchain coupling is much greater in $(SN)_x$ than in either of the $(CH)_x$ isomers. This is due mostly to the greater spatial extent in all directions of the sulfur orbitals *vis-a-vis* carbon.

The role of unit cell symmetry and the associated electron count cannot be overemphasized in discussing the design of a semiconducting or conducting polymer. One further example is given by the speculative structure shown in Fig. 13 for polypyrrole, a material found to be quite conducting when highly oxidized [12]. Note that each pyrrole group is related to its neighbor by screw symmetry. Figure 14 gives its band structure as calculated in the MWH approximation. The result is quite similar to that for a *cis*-$(CH)_x$ chain. Once more the band dispersions are high, especially above and below the 2.5 eV gap. A calculation performed on the –C–C–N–C–C–N– "spine" in Fig. 13, in which the bonds normally connecting to the rest of each pyrrole group were terminated with H atoms, resulted in a band structure very similar to Fig. 14. This strongly suggests that transport will take place along the central backbone rather than around the pyrrole groups.
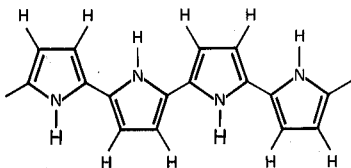

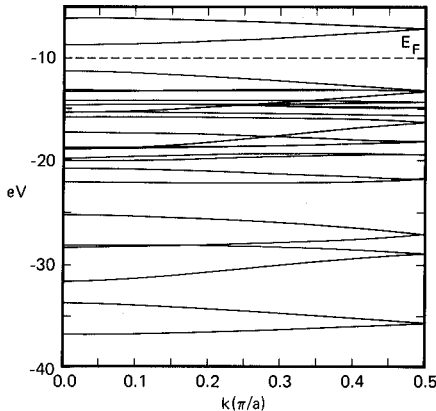Fig. 13. Speculative structure for the polypyrrole chain.

Fig. 14. Band structure of polypyrrole in the chain conformation of Fig. 13.

Recently, Shacklette *et al.*, [13] have reported the synthesis and properties of poly(*p*-phenylene), both doped and undoped. Figure 15 shows the suspected chain structure of this material. Planarity of the phenyl groups is assumed although it is known not to exist for the low molecular weight oligomers of poly(*p*-phenylene). Note that the unit cell symmetry contains no screw axis operation. This fact, coupled with the even electron count, implies that poly(*p*-phenylene) should be an insulator, as is observed. On the other hand, given the planar structure of the chain, and because unit cell bond lengths fall in the range bracketed in Fig. 4, large π-overlap and delocalization are to be expected, resulting in good intrinsic carrier mobility for both holes and electrons. These considerations are confirmed by the results of the 1D MWH band structure calculations for poly(*p*-phenylene) shown in Fig. 16. The zone center band gap is roughly 2 eV and the electron/hole effective mass magnitudes are about 0.5 for the states surrounding the gap. The gap itself is intermediate between *cis*-$(CH)_x$ and polypyrrole and the effective masses close to what would be expected from Fig. 5.

From the lessons of Figs. 4 and 5 it would not be surprising to find little difference in the dynamical transport properties amongst all π-bonded chain systems involving overlap between 2p orbitals. Our calculational results for $(CH)_x$, $(SN)_x$, polypyrrole and poly(*p*-phenylene) support this expecta-
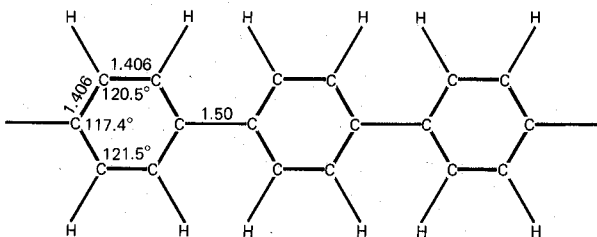

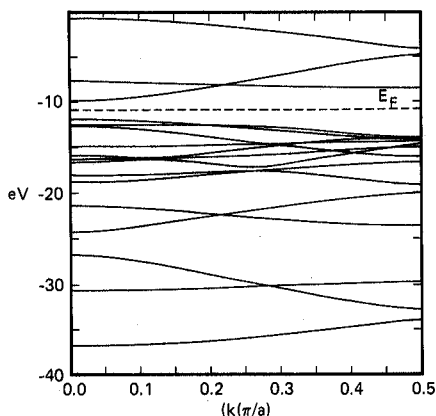Fig. 15. Chain structure of poly(*p*-phenylene) after ref. 13.

Fig. 16. Band structure of a poly(p-phenylene) chain in the MWH approximation. The bond lengths in the phenylene ring were taken to be equal to 1.4 Å long and the bond between rings as 1.5 Å.

tion, which is also borne out experimentally. On the other hand, the one-electron band gap, and thus the optical properties, are somewhat more sensitive to local bond order and length, and especially to symmetry conditions as seen from $trans$-$(CH)_x$ and $(SN)_x$. The claim is often made that synthetic organic chemistry offers a high degree of flexibility in tailoring the properties of materials. However, it is unlikely that much more can be done in scaling the intrinsic transport properties of π-bonded hydrocarbon chains through the introduction of new but similar structures. The experience with existing compounds already bears this out. Certainly, the large changes one achieves in the transport and optical properties of inorganic metals and semiconductors by isostructural substitution of elements vertically in the Periodic Table are not likely to be duplicated in the case of organic polymers. Only great increases in three-dimensional interaction on a local scale would bring about appropriately large changes in the transport properties, and the possibility of cooperative phenomena such as superconductivity and magnetic order.

The application of one-electron theoretical concepts to π-bonded polymers has been the central theme of this paper. It seems likely that the theory can provide a reasonable zeroth-order framework for their transport properties upon which more elaborate models, involving the creation and motion of Pople–Walmsley defects or π-phase kinks, can be built. In this respect, the single-particle picture affirmatively answers the first question posed at the beginning of this paper. The results of recent valence band XPS measurements lend support to this conclusion. In a photoemission measurement, electrons are ejected from the sample leaving behind empty valence band states. If correlation effects predominate in these states, relaxation into a configuration different from the original ground state will occur. In other words, if the hole created by the photoexcitation process remains localized, instead of diffusing its charge density over several unit cells, the resulting Coulomb forces

bring about a renormalized ground state. On the other hand, if delocalization of the valence band hole occurs, the renormalization effects are weak and the photoemission spectrum reflects, to first order, the unperturbed ground state single-particle density-of-states. In Fig. 17 we show the results of several photoemission yield experiments and density-of-states calculations. The curves labelled UPS and CNDO are taken from Duke *et al.* [20]. The former is the ultraviolet photoemission spectrum of polyacetylene, which we assume to be *trans*-(CH)$_x$ although the sample structure is not specifically mentioned in their paper. The latter is the density-of-states obtained from a CNDO calculation on a *trans*-(CH)$_x$ cluster approximately eight units long [20]. The curves labelled XPS and ETB represent data [40] from the valence band X-ray photoemission spectrum on *trans*-(CH)$_x$ and the density-of-states arising from the *trans*-(CH)$_x$ ETB band structure [6] shown in Fig. 7(b), respectively. The XPS, UPS and CNDO curves have been shifted so that the threshold lines up with the valence band edge of the ETB calculation. Admittedly, such a procedure may be rather cavalier; our principal physical justification is that the yield thresholds must necessarily coincide, regardless of any agreement or disagreement throughout the rest of the spectrum. Before comparing experiment with theory, we must comment on what appears to be a great disparity between the UPS and XPS results. This disparity is due to the differences in cross-section of various orbital levels with respect to the kinetic energy of the photoemitted electron. The differences in cross-section between s and p-like states are more readily apparent in UPS than XPS. In UPS, this cross-section difference results in weak structure from the C(2s) states, whereas in XPS the p and s photoyields are more in balance. We identify the XPS structure between —2 and —10 eV as arising from p-states joined by an admixture of s-states at lower energies. Below —10 eV the bands derive al-
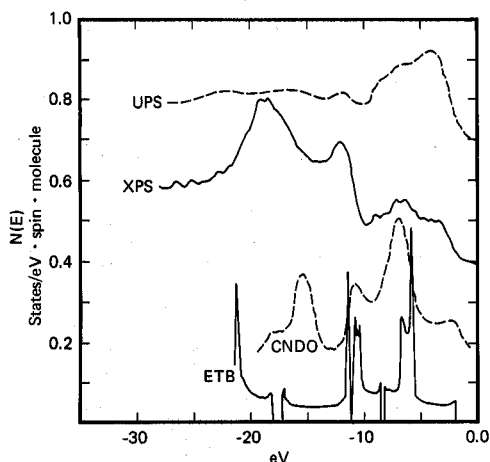

Fig. 17. Photoemissive yields and densities-of-states of *trans*-polyacetylene. The UPS and CNDO are taken from ref. 20. The scales refer only to the calculated ETB density-of-states. The XPS results are due to Brundle [40] and the ETB density of states curve is reproduced from ref. 6.

most completely from 2s states and we assign the −12 and −18 eV structure to critical points in these bands. On the other hand, while there is agreement between the CNDO and XPS at higher energies nearer the Fermi level, it is difficult to reconcile the −15 eV peak in the CNDO calculation with the experimental data. We believe the good agreement between XPS and ETB further substantiates the one-electron model for the ground state of $(CH)_x$. As to its application to the excited state optical properties of $(CH)_x$, the second question posed at the beginning of the paper, the answer is not yet clear and some controversy surrounds both the experimental data and its interpretation. The photovoltaic effect [29] places the excitation energy for free electron–hole pairs (the operational definition of the band gap in a semiconductor) at 1.5 eV. On the other hand, it is reasonable to expect excitons to play some role, perhaps with respect to the optical creation of a Pople–Walmsley defect. That is, one can conceive of a change in bond alternation brought about by an excitonic transition. Complicating matters is the strong energy dependence of the dipole transition probability between π-bonding and antibonding bands [41]. To date, no clear experimental evidence is available as to the existence or non-existence of excitons in polyacetylene, although their presence is theoretically predicted [42]. As mentioned in the opening paragraph of this paper, more optical data and more refined theoretical models are required before a complete picture of the optical properties of polyacetylene can be said to exist.

Acknowledgements

References

1 L. G. S. Brooker, *Rev. Mod. Phys.*, 14 (1942) 275; B. Hudson and B. Kohler, *Annu. Rev. Phys. Chem.*, 25 (1974) 437.
2 H. C. Longuet-Higgins and L. Salem, *Proc. R. Soc. London, Ser. A*, 251 (1959) 172.
3 M. Tsuji, S. Huzinaga and T. Hasino, *Rev. Mod. Phys.*, 32 (1960) 425.
4 J.-M. Andre and G. Leroy, *Int. J. Quantum Elect.*, 5 (1971) 557.
5 M. Kertész, J. Koller and A. Azman, *J. Chem. Phys.*, 67 (1977) 1180; M. Kertész, *Chem. Phys.*, to be published.
6 P. M. Grant and I. P. Batra, *Solid State Commun.*, 29 (1979) 225.
7 T. Yamabe, K. Tanaka, H. Terama-e, K. Fukui, A. Imamura, H. Shirakawa and S. Ikeda, *Solid State Commun.*, 29 (1979) 329.
8 D. J. Berets and D. S. Smith, *Trans. Faraday Soc.*, 64 (1968) 823.
9 C. K. Chiang, C. R. Fincher, Y. W. Park, A. J. Heeger, H. Shirakawa, E. J. Louis, S. C. Gan and A. G. MacDiarmid, *Phys. Rev. Lett.*, 39 (1977) 1098.
10 R. L. Greene, T. C. Clarke, W. D. Gill, P. M. Grant, J. F. Kwak and G. B. Street, *Molecular Metals*, Plenum Press, 1979, p. 203.

11 T. C. Clark, R. H. Geiss, W. D. Gill, P. M. Grant, J. W. Macklin, H. Morawitz, J. F. Rabolt, D. Sayers and G. B. Street, *J. Chem. Soc., Chem. Commun.*, (1979) 332.

12 K. K. Kanazawa, A. F. Diaz, W. D. Gill, P. M. Grant, G. B. Street, G. P. Gardini and J. F. Kwak, *Synthetic Metals*, 1 (1979/80) 329.

13 L. W. Shacklette, R. R. Chance, D. M. Ivory, G. G. Miller and R. H. Baughman, *Synthetic Metals*, 1 (1979/80) 307.

14 Y. W. Park, A. Denenstein, C. K. Chiang, A. J. Heeger and A. G. MacDiarmid, *Solid State Commun.*, 29 (1979) 747. The claim of Park *et al.*, of a sharp metal–insulator transition at 2 at.% iodine has been recently called into question by G. Mihaly, G. Vaucso, S. Pekker and A. Janossy, submitted to *Synthetic Metals*.

15 J. A. Pople and S. H. Walmsley, *Mol. Phys.*, 5 (1962) 15.

16 M. J. Rice, *Phys. Lett. A*, 71 (1979) 152.

17 W. P. Su, J. R. Schreiffer and A. J. Heeger, *Phys. Rev. Lett.*, 42 (1979) 1698.

18 A. A. Ovchinnikov, I. I. Ukrainskii and G. V. Kventsel, *Sov. Phys. Usp.*, 15 (1973) 575.

19 I. A. Misurkin and A. A. Ovchinnikov, *Russ. Chem. Rev.*, 46 (1977) 967.

20 C. G. Duke, A. Paton, W. R. Salaneck, H. R. Thomas, E. W. Plummer, A. J. Heeger and A. G. MacDiarmid, *Chem. Phys. Lett.*, 59 (1978) 146.

21 J. C. Slater, *Phys. Rev.*, 81 (1951) 385; W. Kohn and L. J. Sham, *Phys. Rev. A*, 140 (1965) 1133.

22 A. W. Overhauser, *Phys. Rev. B*, 3, (1971) 1888.

23 A. B. Kunz and T. C. Collins, *J. Phys. B*, 7 (1974) L69.

24 This approximation is often erroneously referred to as the extended Hückel method. It is actually based on a theorem derived by Mulliken for the expectation value of an operator in an LCAO representation. For a discussion of the technique and some applications, see S. P. McGlynn *et al.*, *Introduction to Applied Quantum Chemistry*, Holt, Rinehart and Winston, 1972, Ch. 4.

25 R. Silbey, J. Jortner, S. A. Rice and M. T. Vola, *J. Chem. Phys.*, 42 (1965) 733.

26 A. J. Berlinsky, J. F. Carolan and L. Weiler, *Solid State Commun.*, 15 (1974) 795.

27 F. Herman, D. R. Salahub and R. P. Messmer, *Phys. Rev. B*, 16 (1977) 2453.

28 P. M. Grant (unpublished calculations). This same number can be inferred from the $(SN)_x$ band structure in ref. 39.

29 T. Tani, P. M. Grant, W. D. Gill, G. B. Street and T. C. Clarke, to be published in *Solid State Commun.*

30 C. R. Fincher, M. Ozaki, M. Tanaka, D. Peebles, L. Louchlan, A. J. Heeger and A. G. MacDiarmid, *Phys. Rev. B*, 20 (1979) 1589.

31 H. Kuhn, *Helv. Chim. Acta*, 31 (1948) 1441; H. Kuhn, *J. Chem. Phys.*, 17 (1949) 1198; H. Kuhn, *Helv. Chim. Acta*, 34 (1951) 1308.

32 R. E. Peierls, *Quantum Theory of Solids*, Oxford University Press, London, 1955; H. Froehlich, *Proc. R. Soc. London, Ser. A*, 223 (1954) 296.

33 I. B. Goldberg, H. R. Crowe, P. R. Newman, A. J. Heeger and A. G. MacDiarmid, *J. Chem. Phys.*, 70 (1979) 1132.

34 Y. Tomkiewicz, T. D. Schultz, H. B. Brom, T. C. Clarke and G. B. Street, *Phys. Rev. Lett.*, 43 (1979) 1532.

35 L. Salem, *The Molecular Orbital Theory of Conjugated Systems*, W. A. Benjamin, New York, 1966, Ch. 8.

36 R. H. Baughman and S. L. Hsu, *J. Polym. Sci.*, 17 (1979) 185; R. H. Baughman, S. L. Hsu, G. P. Pez and A. J. Signorelli, *J. Chem. Phys.*, 68 (1978) 5405.

37 C. M. Mikulski, P. J. Russo, M. S. Saran, A. G. MacDiarmid, A. F. Garito and A. J. Heeger, *J. Am. Chem. Soc.*, 97 (1975) 6358.

38 W. E. Rudge and P. M. Grant, *Phys. Rev. Lett.*, 35 (1975) 1799.

39 I. P. Batra, S. Ciraci and W. E. Rudge, *Phys. Rev. B*, 15 (1977) 5858.

40 C. R. Brundle, unpublished data.

41 P. M. Grant, *Bull. Am. Phys. Soc.*, 24 (1979) 327.

42 N. A. Cade, *Chem. Phys. Lett.*, 53 (1978) 45.